DAEHAN HWAHAK HWOEJEE
(Journal of the Korean Chemical Society)
Vol. 18., No. 6, 1974
Printed in Republic of Korea

금속 코발트의 부식과 부동화에 관한 연구

千 井 鈞·白 雲 基

서강대학교 이공대학 화학과

(1974. 8. 29 접수)

A Study on Corrosion and Passivation of Cobalt

Jung-kyoon Chon and **Woon-kie Paik**

Department of Chemistry, Sogang University, Seoul, Korea

(Received Aug. 29, 1974)

요 약. 금속 코발트의 부식과 부동화현상들을 전기화학적 실험방법들을 써서 연구하였다. Tafel slope, Flade potential의 pH의존도, 부식속도의 반응역학적 데이타등으로 부터 코발트와 붕산염완충용액 사이 계면에서 일어나는 부식과 부동화 과정들의 매카니즘을 도출하였다. 금속표면에 흡착된 히드록실기가 표면산화와 부동화막의 형성에 참여하는 것으로 나타났다. 표면막의 성장속도에 관한 데이타로 보아 부동화피막은 "전기장에 의한—이온—이동" 과정에 의하여 성장하는 것으로 보인다. 측정된 표면막의 두께는 약 10 Å에서 20 Å에 이르렀다.

Abstract. Corrosion and passivation of metallic cobalt was studied by means of electrochemical experiments including potentiostatic and galvanostatic measurements and cyclic voltammograms. The mechanisms of active dissolution and passivation of cobalt at the metal/borate buffer solution interface are deduced from the Tafel slope, pH dependence of the Flade potential, and dissolution kinetic data. Hydroxyl group adsorbed on cobalt surface seemes to participate in surface oxidation and formation of the passive layer. The growth kinetic data as measured by the current density suggests a mechanism in which the growth of the passive layer is determined by field-assisted transport of ions through the layer. Thickness of the passive layer was estimated by coulometry to be about 10 Å at the lowest passive potential and to grow gradually with anodic potential to about 20 Å.

Introduction

Experimental studies on corrosion and passivation of metallic cobalt at ordinary temperatures have been sparse compared to those of other ferrous metals.[1~7] Byers and Thing[8] found that cobalt as an anode becomes passive at a higher current density than that required by other ferrous metals.

Electrochemical studies on cobalt by Hickling,[9] Heusler,[10] Iofa, *et al.*,[11] and Kravtsov, *et al.*[12] indicated possible presence of various oxides or hydoxides in the processes of oxidation and passivation of cobalt. Thickness and the optical

properties of the passive film on cobalt surface was measured in a recent study[13] by an optical technique(ellipsometry).

In the present investigation the electrochemical quantities of the corrosion and passivation processes of cobalt electrodes in neutral boric-borate buffer solutions were measured and analyzed in order to elucidate the mechanisms of anodic dissolution, passivation, and film-growth processes, and to find the nature and composition of the passive film.

Experimental

Materials and Chemicals. A smooth electroplated cobalt was used as a specimen. The electroplated specimen was prepared on a platinum wire in a manner similar to those recommended for plating of cobalt[10] and other metals.[14] The thickness of the electroplated cobalt was about 300 μ. The specimen was electropolished to obtain a smooth surface in the plating bath at the anodic current density of 1 A/cm^2 for a few seconds. After the specimen was withdrawn from the bath, it was immediately degreased by washing with isopropyl alcohol followed by washing with a stream of doubly distilled water. All the electrolyte solutions were prepared from doubly distilled water whose specific conductance was less than 10^{-7} ohm^{-1} cm^{-1}. Chemicals of Baker's analyzed reagent were used. Buffer solutions were obtained by mixing 0.15 *N* boric acid solution and 0.15 *N* sodium borate solution.

Cell The pyrex-glass electrolytic cell(*Fig.* 1), having a capacity of about 100 m*l*, consisted of two compartments, one for the specimen and reference electrodes and the other for the counter electrode.

Dissolved oxygen and other gases in the solution were removed by bubbling purified nitrogen gas. The nitrogen gas was passed, before entering the cell, through a nitrogen purifier column(*A*) of fine copper wire heated to 450~500 °C and through a presaturator column (*B*) of distilled water to saturate the gas with water vapor. All the experiments were carried out in this purified nitrogen atmosphere at room temperature. Other impurities in the electrolyte solution were carefully removed by pre-electrolysis between two gold electrodes each of about 10 cm^2 having potential difference of 1.5 volts in the pre-electrolysis cell(*C*) for about 12 hrs before the solution was introduced into the main parts of the cell. Column *C* was connected by ball-joints with other parts, so that the solution could be introduced into the cell by inverting the column upside down.

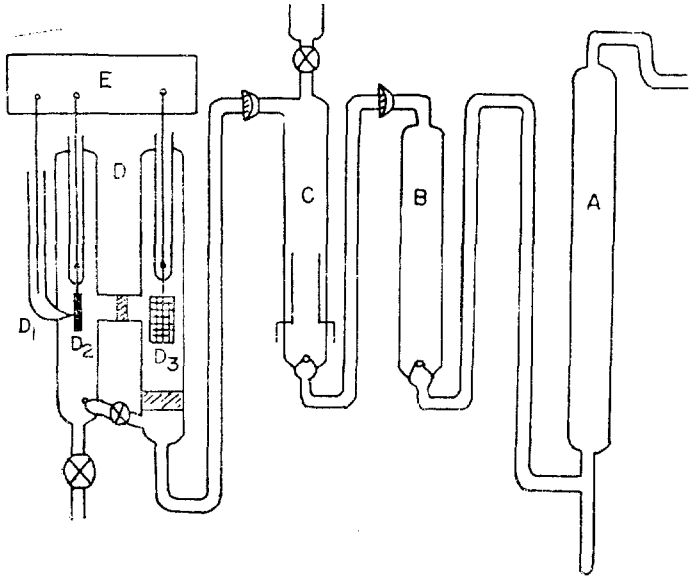

Fig. 1. Experimental cell and accessories. *A*, nitrogen purifier; *B*, presaturator; *C*, pre-elctrolysis cell; *D*, cell; D_1, Luggin capillary and reference electrode; D_2, working electrode; D_3, counter electrode; *E*, potentiostat/galvanostat.

Chloride ions diffusing from the calomel electrode as well as the IR drop in the solution could be avoided by employing a Luggin capillary, D_1,

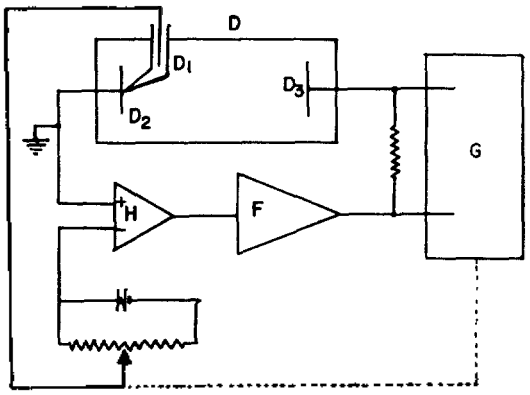

Fig. 2. Electronic circuit for potentiostatic experiment. *D*, cell; D_1, Luggin capillary and reference electrode; D_2, working electrode; D_3, counter electrode; *F*, booster amplifier; *G*, recorder; *H*, differential amplifier.

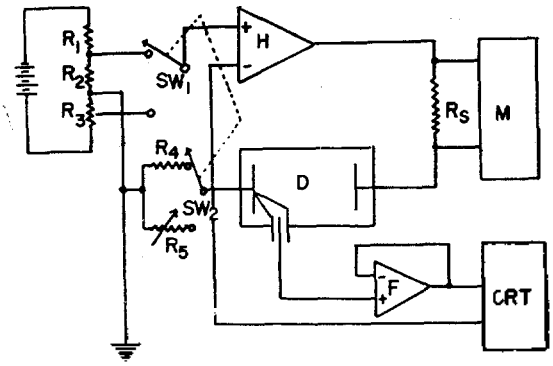

Fig. 3. Electronic circuit for galvanostatic transient measurement. *D*, cell; *F*, potential follower; *H*, differential amplifier; *M*, electrometer; *CRT*, oscilloscope; R_1 to R_5, resistors; R_s, standard resistor; SW_1 and SW_2 synchronized switches.

filled with the same electrolyte as the solution in the cell.

Electrical Circuit. Schematic diagrams of the electronic circuit used in potentiostatic and galvanostatic transient experiments are shown in *Fig.* 2 and 3, respectively.

In the potentiostatic experiments, the change of current with time was recorded by feeding the potential difference across a standard resistor in the current circuit into a high input impedance recorder while the potential of the cobalt electrode with respect to the solution was controlled by an elctronic potentiostat(*Fig.* 2).

The galvanostatic experiments were conducted by using the potentiostat whose input stage is modified as in *Fig.* 3. By operating the synchronized switches, SW_1 and SW_2, current was changed from a fixed value of cathodic current to the desired level of anodic current in a time shorter than a millisecond. The potential difference between the cobalt and the reference electrode was observed on the oscilloscope, *CRT*, through a voltage follower *F* whose input impedance is about 10^{14} ohms(FET input stage) and whose response was faster than a millisecond(nominal rise time of the amplifier is 0.3microsecond). All the potential data given here are referred to the saturated calomel electrode(SCE).

Colorimetric analysis of the solution for cobalt by the Nitroso-*R*-Salt method[15] was carried out after desired period of time of polarization by removing a sample quickly from the solution while the polarization was going on. The limiting sensitivity of this method was about 0.05 μg Co^{2+} in the entire solution.

Results

Anodic Polarization Curve. *Fig.* 4 shows the stationary anodic polarization curve of cobalt obtained by means of the potentiostatic method in a borate buffer solution of pH=8.90. Before making measurement for each point, the cobalt specimen was pretreated with a cathodic current of about 20 $\mu A/cm^2$ for enough time until the surface oxide film was completely removed. Each point of the stationary state polarization curve was taken by applying a constant potential for about one hour until the current density

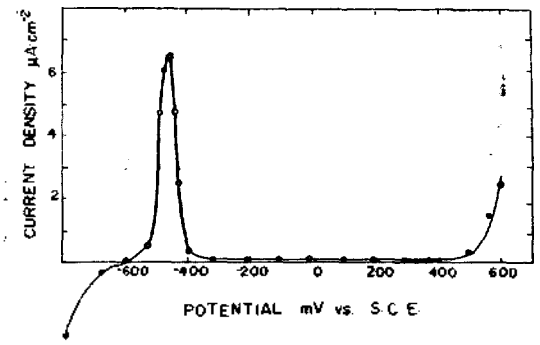

Fig. 4. Steady state polarization curve of cobalt in a solution of pH=8.90.

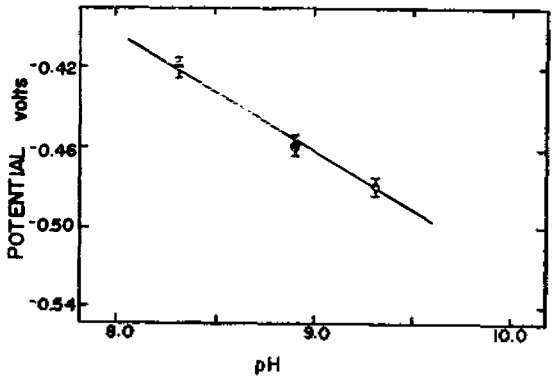

Fig. 5. Effect of pH on the Flade potential.

became steady(refer to *Fig.* 7). The transition from the active dissolution to the passive state took place in the potential range from −0.6 to −0.4 volts. In the passive potential region from −0.4 to +0.5 volts, the dissolution current fell to less than 0.1 $\mu A/cm^2$ after 1 hr of polarization, and was almost constant. In this region the amount of Co^{2+} ions dissolved into solution increased slightly for a few minutes, but no further significant change was observed thereafter. Beyond the potential of +0.5 volts the current again began to increase steeply with rising potential due to rapid dissolution of the metal and oxygen evolution.

Flade Potential and Its pH Dependence. In the potential range where transition takes place from the active to the passive state, the amount of Co^{2+} ions dissolved into solution was also analyzed. At potentials more positive than the peak potential(*Fig.* 4) which is denoted by E_F, the current density decreased sharply and so did the conceatration of the cobalt(II) ions in the solution. The Flade potential, E_F, changed with pH of the solution, and was not significantly influenced by roughness of the electrode. In *Fig.* 5. the pH denpendence of E_F, dE_F/dpH, was observed to be about −60 mV.

Coulometric Measurement of the Thickness of Film. The amount of charge, Q, used in oxidation was measured by recording the current after applying a constant potential in the passivating range on the cobalt whose surface had been completely reduced. The amount of charge passed during 1 hr of polarization was calculated at each potential by graphic intergration of the recorded curve. The equivalent charge for the amount of Co^{2+} found in the solution is then subtracted from the total amount of charge(dotted line in *Fig.* 6) to obtain the amount of charge used in the formation of the film(solid line). The reproducible range in the measurement of the charge was about ±6% along the solid line in *Fig.* 6. The reported density of CoO is 6.45 g cm^{-3}.[16] The film was assumed to be CoO(see discussion section, *nature of the film*) to calculate the thickness at each potential, the result of which is shown also in *Fig.* 6. The amount of Co^{2+} ions in the solution which resulted from dissolution of cobalt below −0.2 volts was larger at lower potentials. In the range between −0.2 and +0.5 volts the relation between Q and E was nearly a straight line having a slope of 0.32 mC·cm^{-2} per 100 mV. It is seen that the thickness of the film is a linear function of potential. There are slight positive and negative deviations from the linear relationship at the potentials of about 0.1 and 0.3 volts, respectively. This suggests partial tran-

sitions of cobalt oxide to higher oxidation states as confirmed by cyclic voltammograms(*Fig.* 9). The thickness thus obtained agrees with that obtained by Paik and Bockris[13] using ellipsometry at −80 mV, 13±1 Å.

The current-time relationships obtained at four passive potentials are shown in *Fig.* 7. The initial parts of the curves are straight lines of slope approximately 45° indepedent of applied potential. Therefore, the experimental relation between the decreasing current, i, and time, t, is

$$\log i = C - \log t \qquad \text{(A)}$$

except after a long time when the relation becomes obscure due to residual current.

Galvanostatic Transient Measurements. The curve of charging potential-time(E-t) transient following the current jump from cathodic 0.1 μA to a desired anodic current, rose initially abruptly and then slowly, and eventually levelled off. The almost linear slope of the initial potential-time curve corresponds to charging of the double layer capacitance of the cobalt/electrolyte interface. Toward the end of the double layer charging, the slope of the potential-time curve became small due to onset of the oxidation. Linear extrapolations of this section and the initial double layer charging section were made. The point where the two extrapolated lines intersect was taken to

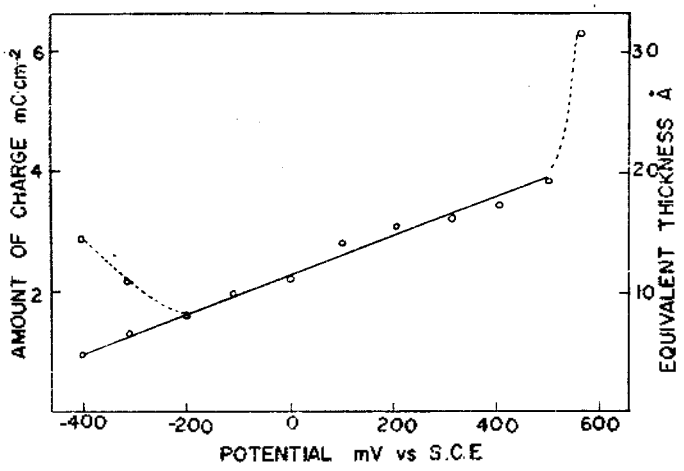

Fig. 6. Coulometric oxidation charge and estimated thickness of passive layer, pH=8.90.

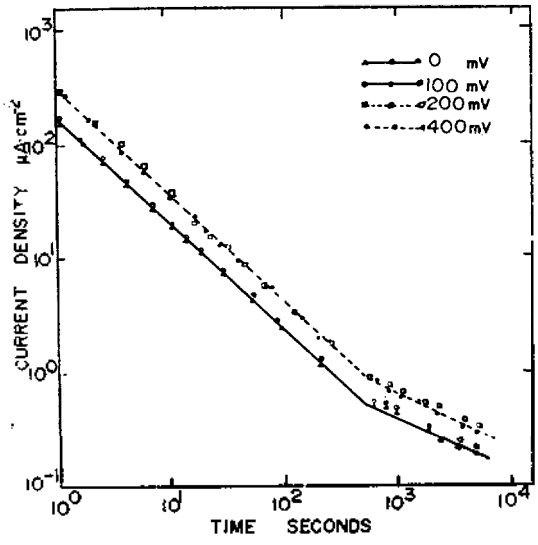

Fig. 7. Change of oxidation current with time in pa ssive region of potential.

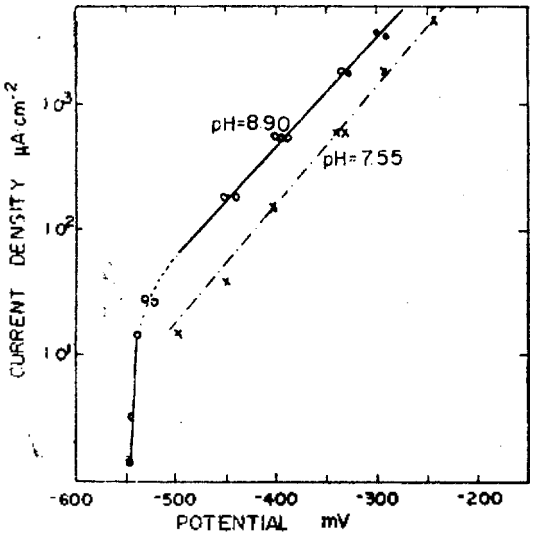

Fig. 8. Initial current density-potential relationship for cobalt.

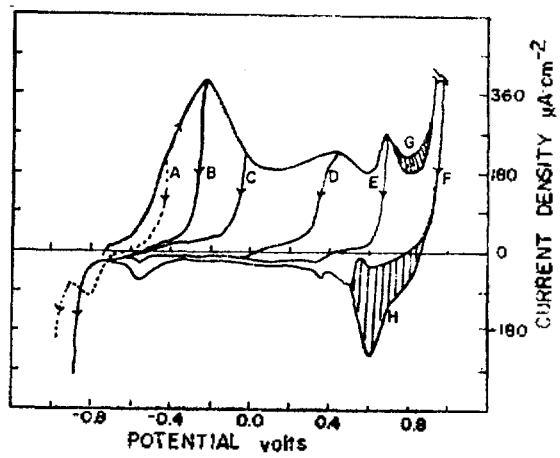

Fig. 9. Cyclic voltammograms, pH=8.90, scan rate=2 volts/min, within the various potential ranges (*A* to *F*).

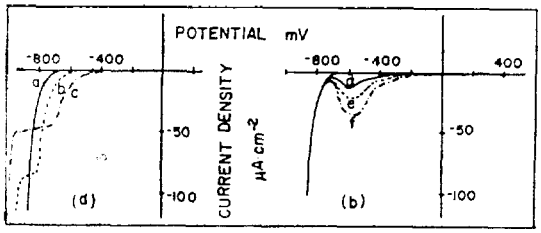

Fig. 10. Effect of anodic polarization and duration of polarization on the cathodic reduction curve of *Fig.* 9. scan rate=2 volts/min. (*a*) $E=-200$ mV, $t=20$ min and $E=400$ mV, $t=2$ hrs; *b*) $E=-200$ mV, $t=5$min; (*c*) $E=-400$ mV, $t=5$ min; (*d*) $E=+300$ mV, $t=5$ min; (*e*) $E=+400$mV, $t=5$min; (*f*) $E=+500$mV, $t=5$min.

give the potential of the oxide-free surface at the imposed current density. The relation between the potential obtained in this way and the current density gives linear Tafel plots as presented in *Fig.* 8. The Tafel slopes are about 140 mV.

Cyclic Voltammogram. The cyclic voltammograms that are shown in *Fig.* 9. were obtained with scan rate of 2 volts/min in the buffered solution of pH=8.90 within the range of -1.0 to $+1.0$ volt. In the cyclic voltammogram obtained by sweeping the full range of potential, there are multiple waves in both the oxidation and reduction sides. In the potential region from 0.60 to 0.80 volts, the oxidation and reduction waves oscillated within certain limits. Reduction voltammograms obtained by starting from various passivating potentials, are represented in *Fig.* 9. by the curves, *A* to *F*. There are subtle differences among the curves on the cathodic side at about -0.8 volt. To see if the differences result from different duration of oxidation times or from the potentials reached in the anodic potential sweep, the potentials reached in the anodic potential was fixed at the peak of curve *A* for various periods before changing to the cathodic direction of potential sweep: the results are in *Fig.* 10(*a*). The gradual change from *c* to *b* to *a* curves resembles the change from *A* to *B* cathodic curves in *Fig.* 9. Thus, the change occurring on the metal surface at anodic potential seemes to take time that depends upon the applied anodic potential. In *Fig.* 9 there are also differences in the height of the reduction waves at about -0.6 volt. To see if these reduction waves are related to the second oxidation wave in the anodic side, the potential sweep was reversed from anodic to cathodic direction from the rising part, from the peak as in curve *D* of *Fig.* 9 and from the falling part of the second anodic wave. The resulting cathodic waves are shown in *Fig.* 10(*b*). From this result, the oxidation product formed with the second anodic wave seems to be reduced at about -0.6 volt.

Discussion

Anodic Dissolution and Formation of Passive Film. The Tafel slope in the passive region of potential, about 140 mV as shown in *Fig.* 8, suggests a single electron transfer in the rate determining step at the initial stage of oxidation. Involvement of hydroxyl ions is evident from the pH dependence of the dissolution rate and Flade potential. The surface reaction can be

reasonably assumed to take place through adsorbed intermediates and to result in a surface layer formed from the adsorbed product. The following mechanism is assumed:

$$Co+OH^- \xrightarrow{R_1} (CoOH)_{ads}+e^- \quad (1)$$

$$(CoOH)_{ads} \xrightarrow{R_2} Co^+ + OH^- \quad (2a)$$

$$2Co^+ \xrightarrow{\text{fast}} Co^{2+} + Co \quad (2b)$$

$$(CoOH)_{ads} \xrightarrow{R_3} CoOH^+ + e^- \quad (3a)$$

$$CoOH^+ + OH^- \xrightarrow{\text{fast}} Co(OH)_2 \quad (3b)$$

$$Co(OH)_2 \xrightarrow{R_4} Co^{2+} + 2OH^- \quad (4)$$

The reactions of (2*a*) and (3*a*) are competitive, but since reaction (3*a*) is strongly potential-dependent, reaction (2*a*) is considered to be dominant in the active dissolution region($E<E_F$) whereas (3*a*) prevails in the passive region ($E>F_F$).

The rate expressions will be:

$$R_1=k_1(OH^-)\exp(\alpha_1 FE/RT) \quad (5)$$

$$R_2=k_2\theta \quad (6)$$

$$R_3=k_3\theta\exp(\alpha_3 FE/RT) \quad (7)$$

where θ is the fractional coverage by the adsorbed intermidiate $(CoOH)_{ads}$, α_1 and α_3 are the transfer coefficients of the reactions (1) and (3*a*), respectively, and F is the Faraday constant. Reactions (2*a*) and (2*b*) together with reaction (1) represent the oxidative dissolution of metal, reactions (3*a*) and (3*b*) correspond to formation of the surface film, whereas R_4 is the rate of film dissolution. For short time polarization, current will be determined by reaction(1). Thus,

$$i_{diss}=k_1'(OH^-)\exp(\alpha_1 FE/RT). \quad (8)$$

If α_1 is considered to be about 1/2,[17] the Tafel slope from equation (8) will be 120 mV, which is close to 140 mV that was observed between about -0.50 and -0.20 volts.

In the active potential region, $R_2 \gg R_3$ and $R_1 \simeq R_2$. Therefore, from equations (5), (6) and (7),

$$\theta=(k_1/k_2)(OH^-)\exp(\alpha_1 FE/RT)$$

$$R_3=(k_1k_3/k_2)(OH^-)\exp\{(\alpha_1+\alpha_3)FE/RT\} \quad (9)$$

R_4 can be taken to be independent of potential as a first approximation if a layer of $Co(OH)_2$ is assumed to be present whereas R_3 is strongly dependent on potential. At a critical potential, E_F, R_3 will become equal to R_4; beyond this potential the surface film can grow in thickness inducing passivity. With $E=E_F$ and $R_3=R_4$ (=constant) equation (9) is rewritten in the logarithmic form,

$$E_F=\frac{-1}{\alpha_1+\alpha_3}(RT/F)\ln(OH^-)+\text{Const.}$$

Assuning that $(\alpha_1+\alpha_3)$ is nearly unity, the pH dependence of E_F will be -60 mV. The observed slope in *Fig.* 5 is in agreement with this prediction.

Nature of the Film. As can be seen from the cyclic voltammograms, *Fig.*9 and 10(*a*), the initially formed oxidation product on the cobalt surface with the first oxidation wave seems to be gradually transformed into another form which is reduced only at more negative potential than the initial form. The transformation was faster at more anodic potential. The initial form might be $Co(OH)_2$ as was supposed above in the film forming reactions, and the second form CoO as was assumed by Heusler.[10] He presumed the transformation was helped by the electric field across the layer. Thus, it is reasonable to expect that the transformation would be faster at higher potentials.

The second and the third oxidation steps are supposed to be partial oxidation of CoO to

Co_2O_3 and oxygen evolution, respectively. Once the oxygen evolution commences, the current density decreases firstly and then fluctuates due to surface blocking by the gas. Co_2O_3 is reduced at about -0.6 V in the cathodic sweep.

Although CoO film is partially oxidized to higher oxidation states at higher anodic potentials, most of the film composition can be represented by CoO. The minimum thickness of this film at the lowest passivating potential (-200mV) is estimated to be about 5 monolayers using the ionic crystal radii.[18]

Film Growth Mechanism. Once the surface oxide starts to grow by reactions (3*a*) and (3*b*), it will soon form a monolayer and eventually grow into multilayer film. The logarithmic growth rate law of equation (A) is considered to be the result of mechanism of film growth by the field-assisted transport of ions across the layer [7a,19];

$$\frac{dL}{dt}=A\exp\left(\frac{\beta V}{L}\right) \qquad (12)$$

where L is the thickness of film and V is the potential difference across the layer. A and β are constants independent of L. Integration of this equation from $t=t_o$ and $L=L_o$ to t and L with the approximation, $\beta V/L\rangle\rangle 1$, is spelled out in the literature[20]: the result is

$$1/L=1/L_o-(1/\beta V)\ln\{a(t-t_o)+1\}$$

where a is a constant. When this result is combined with equation (12)and supposing $dL/dt\propto i$,

$$\log i=\log i_0-\log\{a(t-t_o)+1\}.$$

Here, i_o is the current at the beginning of measurement, t_0. Under the condition, $t\rangle\rangle t_o$, and $at\rangle\rangle 1$, this equation becomes

$$\log i=C-\log t$$

which is the experimentally obtained relation, equation(A).

Acknowledgement

The authors are grateful for the financial support from the Ministry of Science and Technology during 1973.

References

1. Y.M. Kolotyrkin, *Z. Electrochem.*, **62**, 664 (1958).
2. H. Uhling, *J. Electrochem. Soc.*, **108**, 327 (1961).
3. M. Nagayama and M. Cohen, *J. Electrochem. Soc.*, **109**, 781(1962).
4. N. Sato and G. Okamoto. *J. Electrochem. Soc.*, **110**, 605(1963).
5. *a*) J.O'M. Bockris, A.K.N. Reddy and B. Rao, *J. Electrochem. Soc.*, **113**, 1133(1966); b) J.O'M. Bockris, M.A. Genshaw, V. Brusic and H. Wroblowa, *Electrochim. Acta*, **16**, 1859(1971).
6. R.P. Frankenthal, *Electrochim. Acta*, **16**, 1845(1971).
7. a) U.R. Evans, "The Corrosion and Oxidation of Metals," Arnold Publishers, London, 1961; *b*) K.J. Vetter, "Electrochemical Kinetics," Engl. Ed., Academic Press, New York, 1967.
8. H.G. Byers and C.W. Thing, *J. Amer. Chem. Soc.*, **41**, 1902(1919).
9. A. Hickling, *Trans. Faraday Soc.*, **46**, 820(1950)
10. K.E. Heusler, *Corrosion Sci.*, **6**, 183(1966).
11. Z.A. Iofa and Wei Pao-ming, *Russ. J. Phys. Chem.*, Engl. Ed., **36**, 1395(1962).
12. V.I. Kravtsov and O.G. Lokshtanova, *Russ. J. Phys. Chem.*, Engl. Ed., **36**, 1281(1962).
13. W. Paik and J.O'M. Bockris, *Surface Sci.*, **28**, 61(1971).
14. F.A. Lowenheim "Modern Electroplating", 2nd Ed., Wiley, 1963.
15. E.B. Sandell, "Colorimetric Determination of Traces of Metals", Interscience Publishers, New York, 1959.
16. R. C. Wheast, Edit., "Handbook of Chemisty and Physics," Chemical Rubber Co., 1966.

17. N. Tanaka and R. Tamamushi, *Electrochim. Acta*, **9**, 963(1964).
18. L. Pauling, "The Nature of the Chemical Bond", 3rd. Ed., Cornell University Press, Ithaca, 1960.
19. K. Hauffe, "Oxidation of Metals," Engl. Ed., Plenum Press, NewYork, 1965.
20. P. 824 of reference 7*a*